

Toward Hybrid Wi-Fi HaLow Radar CSI Coverage Estimation in Collapsed Structures

Muhammad Faizan Khan^{ID}, Guojun Wang^{ID}, Member, IEEE, Zhigao Zheng^{ID}, Member, IEEE, and Xiangyong Liu^{ID}

Abstract—Wi-Fi sensing has recently gained popularity as it leverages channel state information (CSI) for various applications. Many researchers have studied different sensing applications, from activity recognition to Wi-Fi password cracking. However, there are limited studies on the potential use of Wi-Fi signals in collapsed structures, which could boost rescue operations. Wi-Fi signals at higher frequencies have poor interaction with rubble. However, Wi-Fi HaLow at 902MHz has shown promising results. To achieve reliable sensing, it is crucial to have improved coverage that can effectively measure CSI. Thus, in this study, we propose a state-of-the-art Hybrid Wi-Fi HaLow radar mechanism using Frequency Modulated Continuous Wave (FMCW), Pulse-Doppler (PDR), and Ultrawide Band (UWB) radars. We aim to achieve three objectives: earthquake debris assessment, FMCW, PDR, UWB radar techniques adaptation at 902 MHz, and Hybrid Wi-Fi HaLow radar fusion. Our primary goal is achieved through meticulous site inspections of earthquake-related areas. Subsequently, we convert conventional FMCW, PDR, and UWB signals to Wi-Fi HaLow for optimal debris identification based on the characteristics of the structural engineering involved. Furthermore, we fuse individual signal components to form a comprehensive hybrid Wi-Fi HaLow radar. Based on simulation outcomes, the proposed methodology surpasses previous research and yields promising results.

Index Terms—Wi-Fi HaLow, IoT, hybrid radar, coverage, collapsed structure, rescue.

I. INTRODUCTION

RECENTLY, researchers have been exploring device-free sensing applications that use Wi-Fi radio as sensors on the Internet of Things (IoT) for indoor structures [1], [2]. However, wireless signal penetration is weak in areas like collapsed structures [3], [4], [5]. Investigating low-powered wireless signals that can detect humans under debris is essential for disaster management and aligns with IoT deployment. Therefore, this paper focuses on Wi-Fi HaLow [6], a low-powered Wi-Fi standard designed for IoTs to enhance coverage under debris by presenting a new Hybrid Wi-Fi HaLow Radar system, which addresses weak wireless signals in collapsed

Manuscript received 3 March 2024; revised 25 May 2024; accepted 14 June 2024. Date of publication 18 June 2024; date of current version 11 December 2024. This work was supported in part by the National Natural Science Foundation of China under Grant 62372121, and in part by the National Key Research and Development Program of China under Grant 2020YFB1005804. (Corresponding author: Guojun Wang.)

Muhammad Faizan Khan, Guojun Wang, and Xiangyong Liu are with the School of Computer Science and Cyber Engineering, Guangzhou University, Guangzhou 510006, China (e-mail: csgjwang@gzhu.edu.cn).

Zhigao Zheng is with the School of Computer Science, Hubei Luoja Laboratory, Wuhan University, Wuhan 430072, China.

Digital Object Identifier 10.1109/TCE.2024.3416166

structures. This innovative mechanism overcomes the limitations of traditional radar systems, providing a comprehensive and adaptable sensing solution that can detect structural details and potential signs of life in the future.

Additionally, consumer electronics, such as wearables, smart home devices, and personal health monitoring systems, can leverage Wi-Fi HaLow's low power consumption [7], [8] and extended coverage to operate more efficiently in various environments, including collapsed structures. By incorporating Wi-Fi HaLow, consumer electronics can play a pivotal role in fortifying the IoT ecosystem, ensuring uninterrupted connectivity and functionality in challenging environments [9]. This advancement can significantly enhance the capabilities of consumer electronic devices, underscoring their potential to improve public safety and disaster response efforts, particularly in critical activities such as search and rescue operations.

While this study holds great promise, it also presents significant challenges. These challenges encompass ensuring consistent signal penetration through dense debris, minimizing power consumption [9], [10] while maintaining adequate coverage, and seamlessly integrating the Hybrid Wi-Fi HaLow Radar system with IoT infrastructure and consumer electronics. Addressing these challenges is not just important, but crucial to effectively deploying and succeeding with Wi-Fi HaLow in collapsed structures.

A. Prior Work

Structural collapses due to natural or human-made disasters have been a global concern, resulting in significant loss of lives throughout history [11], [12]. Researchers have explored various techniques to mitigate this issue, including cameras [13], robots [14], [15], sensors [16], [17], UAVs [18], [19], and radars [20], [21], [22]. However, radar-based methods emerged as more promising but are more expensive and sensitive to noise, making them impractical in developing countries with poor infrastructure and low engineering standards. Therefore, there is a need to investigate alternative sensing modalities that can provide accurate and reliable information on the location of individuals in collapsed structures. These modalities should be able to penetrate through debris and provide precise localization information.

Wi-Fi signals present a promising alternative as a sensing modality [23], [24] that is cost-effective, widely available, and can offer various sensing capabilities such as indoor positioning [25], [26], breathing detection [27], [28], security, and privacy [29], [30] via Channel State Information (CSI)

[31] feedback. CSI and Received Signal Strength Indicator (RSSI) are critical metrics in Wi-Fi signals. However, CSI provides detailed channel data, while RSSI only measures total signal power and is widely used for basic signal strength assessment [23], [24]. Hence, Wi-Fi signals can offer a viable solution to rescue operations due to CSI rather than simple RSSI coverage. Nonetheless, extracting useful information from Wi-Fi signals after a disaster can be challenging due to low CSI and environmental factors such as obstacles, attenuation, fading, path losses, and scattering. In the event of a collapsed indoor structure, the situation becomes even more challenging, as roofs, walls, partitions, and doors form multilayered debris [32], [33], making it difficult for wireless signals to penetrate. Thus, enhancing the penetration and strength of Wi-Fi signals under debris is crucial to developing a reliable, cost-effective, innovative solution that can assist post-disaster rescue efforts.

Improving Wi-Fi coverage in collapsed structures entails addressing path loss models and varying Wi-Fi standards. Existing path loss models for collapsed environments, such as for tunnels [34], underscore the complexity of accurately predicting signal behavior using underground sensor networks. However, those path loss models do not suit device-free Wi-Fi sensing in collapsed structures due to the placement of signal emitter outside of the debris and the complexity of the structure. This gap highlights the urgent need for targeted research to develop Wi-Fi-based sensing solutions for disaster scenarios. Moreover, studies indicate that low-frequency wireless signals [5] are more suitable for penetration in such challenging environments, yet few investigations have explored using Wi-Fi radios as sensors. Previous studies [25], [26], [27] have investigated the use of Wi-Fi signals for human detection and localization in indoor environments, laying the foundation for integrating Wi-Fi HaLow signal sensing into radar systems. Although there are limited studies on deploying the Wi-Fi HaLow standard [6], it is the most appropriate solution to ensure sufficient coverage in a simple indoor layout due to operation in a low-frequency band, i.e., Sub 1GHz. Therefore, a more comprehensive coverage estimation of Wi-Fi Halow such as [3] is necessary for collapsed structures.

In addition, recent studies have shown that FMCW [35], [36] and Pulse-Doppler radar [37], [38] are effective for high-resolution imaging and object detection in confined spaces. Furthermore, we also found applications of UWB radar [21] for various sensing purposes. These most common and effective radar-based techniques utilize echo concepts and imaging for rescue operations. However, these methods have not yielded significant results when used to locate individuals under debris due to difficulty in ranging and imaging and hardware costs. Moreover, these radar techniques do not consider wireless sensing, which can lead to ubiquitous solutions. Nevertheless, by combining these techniques and focusing on expanding coverage, it may be possible to enhance weak wireless signals in collapsed structures. Therefore, we envision that integrating these capabilities with the Wi-Fi HaLow frequency band can lead to the development of comprehensive Hybrid radar systems for search and rescue (SAR) operations.

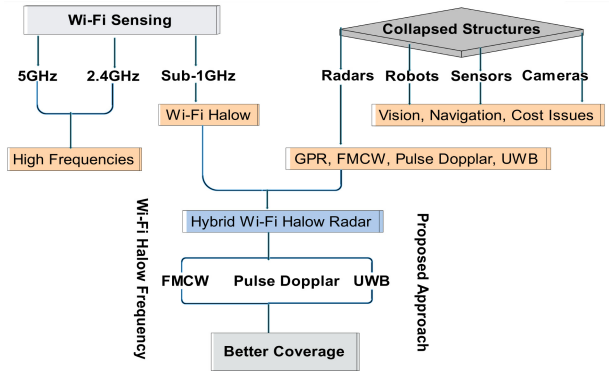


Fig. 1. Towards Hybrid Wi-Fi Halow Radar.

Let us discuss the hybridization of radar technologies for sensing purposes. Studies [39], [40] have explored such ventures, but none of these considered developing a comprehensive system for SAR operations in multilayered collapsed structures, thus providing us with a research gap. Moreover, current radar systems lack the precision required for such complex environments, and a hybrid approach that combines multiple radar types within the Wi-Fi HaLow frequency range is necessary. Therefore, integrating Wi-Fi HaLow signal sensing into radar systems for search and rescue remains worth exploring. Thus, by bridging this gap, we envision advancing the coverage study of Wi-Fi HaLow signals and improving emergency responders' capabilities. Considering this, we aim to propose a comprehensive hybrid Wi-Fi HaLow radar system for multilayered collapsed structures, focusing on real-world applicability and feasibility, as shown in Fig. 1. The hybridization of FMCW, Pulse Doppler, UWB capabilities, and Wi-Fi HaLow signal integration uniquely contributes to better signal coverage under debris. While the individual components of the proposed hybrid radar system have been studied separately, there is a research gap regarding their integration within the Wi-Fi HaLow frequency band for disaster response. Moreover, no other radar type has ever been tested in a hybrid manner or for coverage in collapsed structures.

In summary, developing cutting-edge radar systems for search and rescue missions is paramount, particularly in intricate settings. The suggested hybrid methodology harmonizes FMCW, Pulse Doppler and UWB functionalities within the Wi-Fi HaLow frequency range and incorporates Wi-Fi HaLow signal sensing to maximize the efficacy of radar systems in times of crisis. This study strives to offer a unique and flexible resolution for enhanced situational awareness in multi-tiered, collapsed structures, adding to the ongoing dialogue on radar technology for emergency response.

B. Contribution and Organization

This study aims to develop a hybrid Wi-Fi HaLow radar system for multilayered collapsed structures. Several research questions guide this system's development to meet our objectives, enabling us to integrate FMCW, Pulse Doppler, and UWB radar technologies within the Wi-Fi HaLow frequency band for effective sensing. Firstly, there is a requirement for a site survey to assess the debris from collapsed structures, as it

poses various challenges. Therefore, we conducted case studies of earthquake-hit areas to model the debris and Wi-Fi signal behavior under multilayered rubble. After that, the proposed advanced system accurately assesses earthquake debris in collapsed structures by integrating FMCW, Pulse Doppler, and UWB radar technologies, all optimized for the Wi-Fi HaLow frequency of 902 MHz. Additionally, we explore the integration of Wi-Fi HaLow signal sensing into the radar system to enhance overall situational awareness in collapsed structures. Finally, we simulate a debris model for hybrid Wi-Fi HaLow radar coverage for low-powered wireless across different rubble and signal parameters. Then, we benchmark our work by comparing the results and methodology with existing techniques.

The major contributions of this study are;

- Our study delves into the practicality of utilizing Wi-Fi HaLow signals to ensure sufficient indoor coverage in intricate layouts, such as those found in collapsed structures resulting from earthquakes, tsunamis, or terrorism. Our research specifically focused on earthquake debris, and we conducted case studies of disaster-hit areas. Additionally, we categorized the diverse types of debris as pancake and V-shaped and the materials involved, and analyzed the engineering standards utilized based on our case studies.
- Our approach to addressing the coverage issue involves utilizing a Hybrid Wi-Fi HaLow signal and echo modeling technique based on a debris model developed using case studies. This sophisticated approach allows for a detailed analysis of the structural materials and signal propagation mechanisms. We hypothesize that wireless signals will behave similarly to radar signals, which bounce off objects and provide valuable information for inference.
- After that, we present the Hybrid Wi-Fi HaLow radar mechanism by transforming the traditional FMCW, Pulse-doppler, and UWB radar to operate at 902 MHz and integrate with Wi-Fi HaLow, thereby rejecting noise and clutter. Our proposed approach considers channel stochastic factors, such as scattering, attenuations, and fadings, to have better coverage under multilayered debris. Moreover, we selected a predefined received signal threshold to ensure robust CSI reception for monitoring vital signs in future studies.
- We thoroughly validate our signal propagation models via meticulous simulations, taking into account signal intensities, thresholds, debris types, and layers. In addition, we conduct comparisons between our findings and those of other studies. We conclude that Wi-Fi HaLow signals outperform existing methods utilizing a hybrid radar mechanism. Ultimately, this work holds potential for IoT-based rescue solutions, aligning with the original purpose of Wi-Fi HaLow.

The paper is structured as follows: first, we delve into problem formulation in Section II. Next, we introduce the Hybrid Wi-Fi HaLow radar in Section III, then present simulation results in Section IV. Then, we briefly analyze the research study in Section V and compare its contributions and limitations to existing literature. Finally, Section VI concludes the paper with directions for future research.

II. PROBLEM FORMULATION

This section lays the groundwork for expanding Wi-Fi HaLow signal coverage in collapsed structures. Our approach involves breaking down the problem into three subsections: Firstly, we provide case studies of three earthquake sites and analyze the characteristics of the debris. Next, we evaluate the types of collapsed buildings and develop a layered debris model. Lastly, we introduce the Wi-Fi echo model, which utilizes the Hybrid Wi-Fi HaLow radar method to investigate coverage in collapsed structures.

A. Collapsed Structures Case Studies

The initial step in proposing a solution for enhancing Wi-Fi HaLow signal coverage under debris involves identifying the collapsed structure environment [3] responsible for significant damage, which is prevalent in many developing nations. Disasters can result from various factors, such as war, climate change, fire, earthquakes, and terrorism. However, this article focuses solely on conducting case studies of earthquake sites. This is due to the active fault lines in developing countries, where weak economies result in inadequate adherence to construction standards and building codes. To better understand the impact of debris, we examined two earthquake-affected regions in Afghanistan and Pakistan. Moreover, we also consider a case study for China to discuss the effects on the higher-income economy, but since it's on an active fault line and has faced many catastrophic earthquakes.

1) *Zindeh Jan Earthquake Study*: Zindeh Jan¹ is a quaint town situated in the central region of Herat Province, Afghanistan. It can be found at 34.3456°N 61.7317°E and is located at an elevation of 835 meters, as depicted in Fig. 2a. Unfortunately, the town was severely impacted by four massive earthquakes, each measuring Mww 6.3, and their subsequent aftershocks in early October 2023. The first two earthquakes hit on 7 October, followed by several aftershocks on 11 and 15 October. Two additional magnitude 6.3 earthquakes struck the same area, with thrust faulting being the cause of these events. Tragically, the World Health Organization reported 1,482 fatalities, 2,100 injuries, and 43,400 people affected by these devastating earthquakes.

According to Miyamoto's Herat Earthquake Assessment Report,² an investigative team was dispatched to evaluate 11 villages in the region affected by earthquakes. The report highlights that most structures (90%) were constructed using mud/raw earth and adobe (10%) with substandard building practices, as shown in Fig. 2b. The team identified structural deficiencies, such as insufficient foundations, irregular brick sizes, and poor connections. Additionally, the report warns that using dome roofs up to 40cm thick poses a significant seismic hazard, as shown in Fig. 2c.

2) *Balakot Earthquake Study*: Balakot³ is a small town nestled in the Mansehra district of the Khyber-Pakhtunkhwa province in Pakistan. Located at 34.550842 latitude and

¹https://en.wikipedia.org/wiki/Zendej_Jan

²<https://miyamotointernational.com/2023-herat-afghanistan-earthquake-preliminary-shelter-and-housing-response/>

³<https://en.wikipedia.org/wiki/Balakot>



(a) Location of Zindajan town

(b) Ruins of house

(c) Mapping collapsed materials

Fig. 2. Earthquake Case Study 1: Zindajan Town, Herat Province, Afghanistan. Adapted from URL².

(a) Location of Balakot City

(b) Ruins of market

(c) Mapping collapsed materials

Fig. 3. Earthquake Case Study 2: Balakot City, KPK Province, Pakistan. Adapted from [3], [4].



(a) Location of Yingxiu town

(b) Ruins of school

(c) Mapping collapsed materials

Fig. 4. Earthquake Case Study 3: Yingxiu Town, Wenchuan County, China. Adapted from [3], [4].

73.352957 longitude, as shown in Fig. 3a, it was tragically devastated by a powerful earthquake on October 8, 2005. The quake, measuring 7.6 on the Richter scale,⁴ wrought extensive destruction throughout the town. The earthquake's aftermath was catastrophic, with the Pakistani government reporting that 87,350 people perished, 138,000 were injured, and 3.5 million were displaced. The central market in Balakot was among the areas hardest hit, as the seismic fault line runs through it.⁵

After thoroughly investigating the damaged central plaza, as shown in Fig. 3b, we observed that poor construction worsened the damage and resulted in more casualties in the affected areas. The plaza consisted of substandard construction materials, such as lumber, concrete, and masonry blocks, as shown in Fig. 3c. Most of the civil structures in the area were weak wall constructions based on non-engineered, unreinforced masonry methods. Flat roofs were built of non-machined wood beams and straw-reinforced mud slabs in small adjoining villages. These weak structures were occasionally referred to as "Tayyar Chath."

3) *Wenchuan Earthquake Study:* Our last field study deals with Wenchuan County, a region in southwestern China that

suffered significant damage from a devastating earthquake in May 2008. The epicenter of the quake was Yingxiu, a small town located at 31°03' 32" N and 103°29' 41" E, as shown in the accompanying Fig. 4a. Sadly, the earthquake resulted in over 68,000 casualties and caused extensive destruction to the surrounding rural areas.

A thorough examination of the Xuankou Middle School ruins in Yingxiu town (as depicted in Fig. (4b, 4c)) revealed that the collapse was due to subpar construction materials such as concrete, brick, and lumber and improper building codes creating voids that could trap individuals. Our analysis discovered that the columns, steel bonding, and beam were unreliable and vulnerable to collapse.

B. Debris Pattern

In this part, we map inferences from earthquake case studies to a conceptual layered debris model, as shown in Fig. 5. We classify debris as mud and masonry, where concrete, brick, masonry blocks, and lumber constitute masonry structures. In contrast, rammed-earth, thatch, adobe brick, stone, and lumber are building materials for mud structures. We observed that mud and low-story wall-bearing masonry structures were more prevalent in the Zindeh Jan and Balakot earthquakes. However, the Yingxiu earthquake

⁴<https://earthquake.usgs.gov/earthquakes/eventpage/usp000e12e#executive>

⁵ <http://www.ndma.gov.pk/publications.php>

⁶ <http://www.gsp.gov.pkpublication>

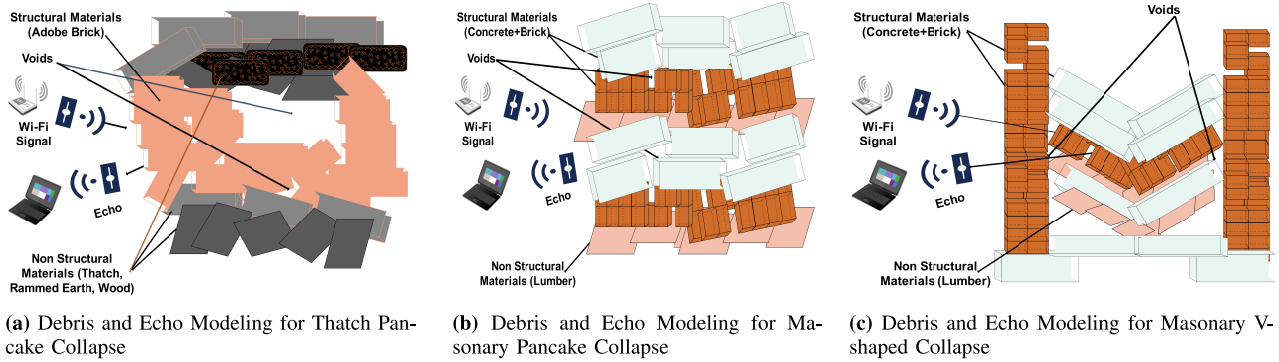


Fig. 5. Debris and Echo Modeling for Collapsed Structures.

revealed multi-story masonry structures with better beams and columns.

Let us thoroughly analyze our established debris model, which we employed in [3]. Debris can be a heap or on a small scale. Therefore, there is a need to classify it into a maximum and minimum layers scenario. Moreover, the enclosed debris area is spread both horizontally and vertically. Due to fewer obstructions and voids, CSI will be stronger in horizontal layers. However, we emphasize vertical-layered rubble, which can entrap humans and cause more damage than horizontal ones.

Furthermore, voids are formed after structural collapse. So, authors in their previous study mapped the possibility of open spaces from debris sites. We observed that the most common debris model is pancake collapse [4], found in all three case studies where the complete failure of columns or load-bearing walls resulted in destruction, as shown in Fig. (5a, 5b). When victims are trapped under a large amount of debris, they struggle to breathe and may not survive for long. Such collapses tend to leave fewer empty spaces. Additionally, our research has revealed that mud and low-masonry structures can experience a V-shaped collapse [4] when the floor remains intact on both sides. In this scenario, the floor caves in at an angle with the lower part of the walls, resembling the shape of a “V,” as depicted in the accompanying Fig. 5c. Fortunately, this type of collapse can create empty spaces where people can be located and rescued if necessary.

C. Wi-Fi HaLow Echo Pattern

Let us consider the Wi-Fi HaLow signal behavior in the above-developed debris model, as shown in Fig. 5. Compared to typical indoor scenarios, collapsed structures present a much more complex challenge due to the intricate layers of debris present from walls, halls, and doors [3]. As a result, wireless signals struggle to penetrate and reflect from the debris, often leading to signal damping due to various fading phenomena. However, there is still a need for an in-depth investigation of Wi-Fi signals as it may turn into a post-disaster SAR solution.

We consider a Wi-Fi HaLow echo model to simplify the coverage computation, as shown in Fig. 6. We assume that wireless signals follow the hybrid radar principle. Our objective is to capture a clear echo amidst the wireless pulses that may bounce off or be absorbed by debris. This will allow us

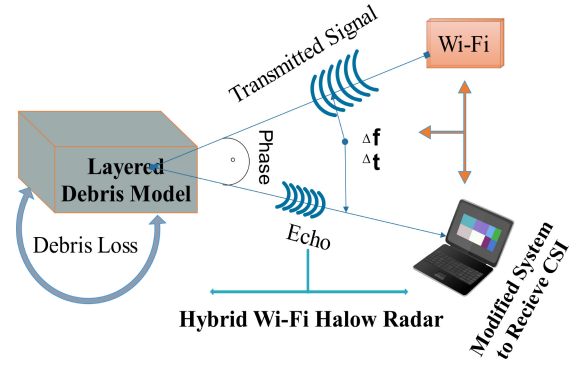


Fig. 6. Hybrid Wi-Fi HaLow Radar Working Principle.

to obtain accurate CSI. We have noticed that a signal strength of -90dBm in typical Wi-Fi sensing applications can provide some CSI. However, our research found that reflections are caused by debris, which may also include background noise and only result in the detection of tiny movements or breathing information in the channel. Therefore, if the signal coverage is strong enough, even with a sensitivity of -90dBm , the resulting reflections will be untrustworthy to extract CSI from the received signal. So, there is a need for a strong echo signal. The echoes must surpass the predetermined threshold (PDT) to achieve the desired outcome. Furthermore, our analysis only considers signals originating from reflected debris while disregarding all other signals as extraneous noise.

In a nutshell, our main objective is better coverage for Wi-Fi HaLow signals from collapsed structures, as these face higher clutter and noise debris. The research intends to fill this gap by proposing a hybrid radar mechanism at Wi-Fi HaLow frequency.

III. PROPOSED APPROACH

This section presents our proposed hybrid Wi-Fi HaLow radar constituent of FMCW, Pulse-doppler, and UWB radar signals in depth, as shown in Fig. 6. Firstly, we discuss individual radar modules and their operation at Wi-Fi HaLow frequency; then, we study the hybrid signal formation, followed by debris losses and CSI consideration.

A. FMCW Module

The hybrid Wi-Fi HaLow radar system's FMCW (Frequency Modulated Continuous Wave) module is essential for sensing objects with high-range resolution within the Wi-Fi HaLow frequency band. Generally, FMCW [41] operates by continuously altering the transmitted signal's frequency over time. Therefore, the FMCW capability is strategically integrated into this proposed hybrid radar system to detect tiny movements or objects within complex collapsed structures. The continuous waveform generated by the FMCW radar allows for detailed mapping of the under-consideration environment, enabling the system to detect subtle changes in range. This ability is precious in cluttered and confined spaces where traditional radar systems may struggle to provide accurate and fine-grained information. Therefore, we envision FMCW capability in the hybrid radar system seamlessly aligning with other sensing modules, such as Pulse Doppler and UWB, ensuring cohesive and complementary functionality.

Step 1: FMCW Signal Generation: Generally, the FMCW signal follows a linear frequency sweep pattern from its starting frequency (f_{start}) to its end frequency (f_{end}) within a specific sweep time (T_{sweep}). This modulation is expressed mathematically as a sinusoidal waveform, which depicts the gradual transition of the signal's frequency over time.

$$s(t) = \sin(2\pi f(t)t) \quad (1)$$

where $f(t)$ is given by through relation of sweep time and frequency boundaries

$$f(t) = f_{\text{start}} + \frac{(f_{\text{end}} - f_{\text{start}})}{T_{\text{sweep}}} t \quad (2)$$

Now, putting $f(t)$ value in (Eq 1)

$$S(t) = \sin\left(2\pi\left(f_{\text{start}} + \frac{f_{\text{end}} - f_{\text{start}}}{T_{\text{sweep}}} \cdot t\right) \cdot t\right) \quad (3)$$

Now, to modify and evaluate the FMCW signal ($S(t)$) in the hybrid Wi-Fi HaLow radar system context, we incorporate an interpolated frequency (interp_freq) from an interpolation function. This ensures a smooth transition between start and end frequencies over the given time range. Moreover, this modification improves the accuracy of the frequency sweep and is essential for realistic radar simulations. The signal frequency can be continuously and precisely adjusted with interpolation during the sweep time. This results in a more precise and reliable radar module detecting even complex, multilayered debris. Initial FMCW signal ($s(t)$) from (Eq 1) can be remodeled as modified FMCW signal ($mfs(t)$);

$$mfs(t) = \sin(2\pi \times \text{interp_freq} \times t) \quad (4)$$

Next, we define (*np.interp*) using attributes of (Eq 2) such as sweep time along with start and end frequency as below;

$$\text{interp_freq} = \text{np.interp}(t, (t.\text{min}(), t.\text{max}()), (f_{\text{start}}, f_{\text{end}})) \quad (5)$$

Now, putting value of interp_freq from (Eq 5) to (Eq 4), we get;

$$mfs(t) = \sin(2\pi \times \text{np.interp}(t, (t.\text{min}(), t.\text{max}()), (f_{\text{start}}, f_{\text{end}}) \times t)) \quad (6)$$

(Eq 6) represents the FMCW transmitted signal from hybrid Wi-Fi Halow radar but lacks stochastic factors.

Step 2: Stochastic Factors in FMCW Signal Propagation: We observe that the Wi-Fi Halow signal penetrating through debris faces severe stochastic attenuation $A(t)$, scattering $S(t)$, and fading $F(t)$ at any given time t , which can be expressed as the sum of respective material-specific coefficients over distance. Let n be the number of material layers. We introduce random variables $\eta_i(t)$, $\xi_i(t)$, and $\zeta_i(t)$ for each material layer i to model the stochastic nature of attenuation, scattering, and fading, respectively.

$$A(t) = \sum_{i=1}^n \eta_i(t) \cdot \alpha_i \cdot t \quad (7)$$

$$S(t) = \sum_{i=1}^n \xi_i(t) \cdot \sigma_i \cdot t \quad (8)$$

$$F(t) = \sum_{i=1}^n \zeta_i(t) \cdot F_i \cdot t \quad (9)$$

where (σ) , (α) , and (F) represent the attenuation coefficient, scattering coefficient, and fading factor, respectively.

Step 3: Incorporating Stochastic Factors in FMCW Signal: Now, we incorporate the stochastic signal factors in (Equation (III-A)), which leads to the resulting FMCW signal as the outcome of the product of these individual elements.

$$R(t) = \sin\left(2\pi\left(f_{\text{start}} + \frac{f_{\text{end}} - f_{\text{start}}}{T_{\text{sweep}}} \cdot t\right) \cdot t\right) \cdot e^{-A(t)} \cdot S(t) \cdot F(t) \quad (10)$$

Giving values to (Eq 10) from (Eqs (7, 8, 9))

$$R(t) = \sin\left(2\pi\left(f_{\text{start}} + \frac{f_{\text{end}} - f_{\text{start}}}{T_{\text{sweep}}} \cdot t\right) \cdot t\right) \cdot \exp\left(-\sum_{i=1}^n \eta_i(t) \cdot \alpha_i \cdot t\right) \cdot \sum_{i=1}^n \xi_i(t) \cdot \sigma_i \cdot t \cdot \sum_{i=1}^n \zeta_i(t) \cdot F_i \cdot t \quad (11)$$

(Eq 11) provides the traditional FMCW signal by employing the stochastic elements $\eta_i(t)$, $\xi_i(t)$, and $\zeta_i(t)$, which contribute to attenuation, scattering, and fading variations. This enables detailed stochastic modeling of signal propagation in complex multilayered debris scenarios.

Now, we improve the FMCW signal equation (Eq 11) to increase the realism of the hybrid Wi-Fi HaLow radar simulation by incorporating the interpolated frequency np.interp() function. To capture the cumulative effects of stochastic elements such as attenuation ($A(t)$), scattering ($S(t)$), and fading ($F(t)$) over time, we multiply them to the signal. This comprehensive modeling accurately reflects the complex nature of multilayered debris scenarios, where the radar signal

experiences various attenuations, scatterings, and fadings as it traverses different material layers.

$$R(t) = \sin(2\pi \times \text{np.interp}(t, (\text{t.min}(), \text{t.max}()), (f_{\text{start}}, f_{\text{end}})) \times t) \times e^{-A(t)} \times S(t) \cdot F(t) \quad (12)$$

Step 4: Wi-Fi HaLow Signal Propagation: We incorporate supplementary elements of randomness to enhance Wi-Fi HaLow signal propagation. Specifically, we take into account variations in transmitted power P_t , antenna gain G_A , and other material-specific parameters as detailed in (Eq 13).

$$\begin{aligned} P_r(t) &= P_t - G_A - 20 \cdot \log_{10}(A(t)) \\ &\quad - 20 \cdot \log_{10}(S(t)) \\ &\quad - 20 \cdot \log_{10}(F(t)) - \text{integrated_signal}[t] \end{aligned} \quad (13)$$

Step 5: Calculate Signal Coverage Range: Finally, we determine the signal coverage range $R_{\text{coverage}}(t)$ based on the received power and distance:

$$R_{\text{coverage}}(t) = P_r(t) - 20 \cdot \log_{10}(t) \quad (14)$$

B. Pulse-Doppler Module

We envision that Pulse Doppler Radar (PDR) technology [42] integrated with Wi-Fi HaLow frequency band can enhance motion detection and target tracking capabilities under collapsed structures. It emits short pulses and filters out static clutter, which can focus on detecting dynamic signals for identifying moving targets like survivors. PDR complements other radar types in the hybrid system, creating a synergistic approach. This adaptability makes it significant for future search and rescue (SAR) solutions. Now, let us transform PDR for the Wi-Fi Halow signal.

Step 1: PDR Signal at Wi-Fi HaLow: We assume the PDR signal is operating at the Wi-Fi HaLow frequency ($f_{\text{wifi-halow}}$). The mathematical modeling of this signal involves the representation of a sinusoidal waveform with the Doppler frequency shift, denoted by $s_{\text{pd}}(t)$, and is given by:

$$s_{\text{pd}}(t) = \sin(2\pi f_{\text{wifi-halow}} t) \cdot e^{j2\pi f_d t}. \quad (15)$$

Here, $f_{\text{wifi-halow}}$ is the Wi-Fi HaLow frequency, and f_d is the Doppler frequency shift introduced by target motion. Now, to account for real debris conditions, we introduce stochastic elements by considering additive white Gaussian noise ($n_{\text{pd}}(t)$). Therefore, the received signal at the Wi-Fi HaLow frequency is re-modeled as below:

$$r_{\text{pd}}(t) = s_{\text{pd}}(t) + n_{\text{pd}}(t). \quad (16)$$

The noise component, denoted as $n_{\text{pd}}(t)$, is an essential factor in the PDR signal that represents the uncertainties and interferences that affect the PDR signal under debris.

Step 2: Multi-Layered Debris for PDR at Wi-Fi HaLow: Now, we extend our modeling to include the transmission of the PDR signal through multilayered debris. The received power ($P_r(t)$) takes into account the effects of attenuation, scattering, and fading caused by the multiple material layers. Therefore, by integrating the scattering coefficient (σ), attenuation coefficient (α), and fading factor (F) into the model, the power received at each layer as a result of Wi-Fi HaLow

signal propagation at the specified frequency ($f_{\text{wifi-halow}}$) will be:

$$\begin{aligned} P_r(t) &= P_t \cdot G_A \cdot \frac{1}{R^2} \\ &\quad \cdot e^{-\alpha R} \cdot e^{-j2\pi f_{\text{wifi-halow}} t} \cdot \sigma R^2 \cdot F \end{aligned} \quad (17)$$

where parameters such as P_t , G_A , α , σ , and F are material and environmental properties. Moreover, R is the distance, and τ , as the round-trip time. To incorporate uncertainties and environmental interference, we introduce noise ($n_{\text{wi-fi-halow}}(t)$) into the received Wi-Fi HaLow signal. The stochastic model is expressed as:

$$r_{\text{wi-fi-halow}}(t) = P_r(t) + n_{\text{wi-fi-halow}}(t). \quad (18)$$

where $n_{\text{wi-fi-halow}}(t)$ represents the noise component for the Wi-Fi HaLow signal.

Step 3: Integrated Signal: The integrated signal ($s_{\text{intg}}(t)$) combines the Wi-Fi HaLow PDR signal with the received Wi-Fi HaLow signal expressed as:

$$s_{\text{intg}}(t) = s_{\text{pd}}(t) + r_{\text{wi-fi-halow}}(t). \quad (19)$$

where $r_{\text{wi-fi-halow}}(t)$ represents the received Wi-Fi HaLow signal. To complete the model, we consider the stochastic aspects of the integrated signal. The overall received signal ($r_{\text{intg}}(t)$) includes noise terms from both the Wi-Fi HaLow pulse-Doppler radar module and the received Wi-Fi HaLow signal:

$$r_{\text{intg}}(t) = s_{\text{intg}}(t) + n_{\text{pd}}(t) + n_{\text{wi-fi-halow}}(t). \quad (20)$$

This derivation integrates PDR with the Wi-Fi HaLow radar system, accounting for multilayered debris effects. The stochastic model includes PDR and Wi-Fi HaLow signal noise terms in the integrated scenario.

C. UWB Module

The Ultra-Wideband (UWB) [43] module in the hybrid Wi-Fi HaLow radar system can enhance sensing capabilities in collapsed structures. It operates across a broad frequency spectrum, offering exceptional imaging and penetration through materials, making it adept at detecting small objects or movements with extraordinary accuracy. We design the UWB module to operate within the Wi-Fi HaLow frequency band, ensuring compatibility with other radar functionalities. The hybrid Wi-Fi HaLow radar system's UWB capability is seamlessly integrated with FMCW and Pulse Doppler functionalities, forming a cohesive sensing solution. The system leverages the strengths of UWB to supplement the high range resolution of FMCW and the motion detection capabilities of Pulse Doppler, creating a well-rounded and adaptable sensing platform.

Step 1: UWB Signal at Wi-Fi HaLow: Since we aim to utilize the UWB radar module for the hybrid Wi-Fi HaLow radar system, the transceiver needs to be modified to operate within the designated frequency range of the 902-928 MHz band. Moreover, we modify the transmitted UWB pulse $h(t)$ to account for the frequency shift and scattering through L layers within the complex multilayered debris environment.

Furthermore, we consider adjusting the attenuation coefficient α_i to match the unique characteristics of Wi-Fi HaLow frequency. Meanwhile, the distance d_i through each layer is also factored in the attenuation term.

$$s(t) = h(t) \cdot \prod_{i=1}^L \exp(-\alpha_i \cdot d_i) \cdot \exp(-j\phi_i) \quad (21)$$

Here:

- α_i is the attenuation coefficient of layer i .
- d_i is the distance through layer i .
- ϕ_i is the phase shift due to scattering in layer i .
- j represents the imaginary unit.

Step 2: Pulse Repetition Frequency (PRF): The pulse repetition frequency (PRF) is a crucial parameter in the UWB radar module, as it determines the rate at which pulses are emitted from transceivers towards debris. Moreover, it ensures precise localization of targets within multilayered debris by providing temporal resolution to the proposed hybrid radar.

$$PRF = \frac{1}{T_{pulse}} \quad (22)$$

Step 3: UWB Signal Through Multilayered Debris: In multilayered debris, UWB signal $x(t)$ can be derived by adding modified pulses with adjustments to Wi-Fi HaLow frequency.

$$x(t) = \sum_{n=-\infty}^{\infty} r(t - n \cdot T_{pulse}) \quad (23)$$

We now incorporate stochastic elements such as scattering, attenuation, and fading factors to represent better how UWB module signals interact with debris scenarios. Moreover, we introduce additive white Gaussian noise (AWGN) term ($n_{uwb}(t)$) to address the uncertainties, interferences, and noises from multilayered debris to ensure reliability.

$$r(t) = g(t) \cdot \prod_{i=1}^L \exp(-\alpha_i \cdot d_i) \cdot \exp(-j\phi_i) \cdot \sigma_i \cdot F(t) + n_{uwb}(t) \quad (24)$$

Here, σ_i and $F(t)$ represents the scattering coefficient and fading factor respectively. Furthermore, we define the Gaussian Probability Density Function (PDF) for signal generation:

$$f(x; \mu, \sigma) = \frac{1}{\sqrt{2\pi\sigma^2}} e^{-\frac{(x-\mu)^2}{2\sigma^2}} \quad (25)$$

Now, this particular function generally denotes the probability distribution of any random signal $x(t)$ produced at each time point t_i . However, when we consider the UWB radar module, the signal is obtained from a standard distribution with a mean (μ) of 0 and a standard deviation (σ) of 1, as presented in Equation (26).

$$\begin{aligned} \text{signal}(t_i) &= \text{random normal distribution with mean } 0 \\ &\quad \text{and standard deviation } 1 \end{aligned} \quad (26)$$

Step 4: UWB Signal Spectrum: Finally, we discuss the UWB module signal spectrum, characterized by the power spectral density ($S(f)$), which considers scattering, attenuation, and fading influences. This spectrum analysis helps to understand the frequency distribution of the UWB signal and how it performs in multilayered debris. Therefore, by integrating the modified UWB radar module with other radar signals like FMCW and pulse-Doppler, the hybrid Wi-Fi HaLow radar system takes a comprehensive approach to coverage analysis in collapsed structures while considering the unique frequency characteristics of Wi-Fi HaLow.

$$S(f) = |\mathcal{F}\{R(\tau)\}|^2 \quad (27)$$

where $R(\tau)$ is the autocorrelation function of $x(t)$.

D. Wi-Fi Halow Hybrid Fusion

Integrating the Wi-Fi HaLow in the proposed hybrid radar system is essential to enhance the overall sensing capabilities in collapsed structures. It can provide high-range resolution and precise detection of small movements or objects under debris. The hybrid model acquires an additional layer of information and context by seamlessly incorporating Wi-Fi HaLow signal sensing into the radar system. The system can offer valuable environmental insights, including electronic devices, potential communication signals, and human presence. The integrated signal is formed by adding these three signals, representing a combined approach to sensing and communication in a complex environment.

$$\begin{aligned} \text{integrated_signal}[i] &= \text{fmcw_signal}[i] \\ &\quad + \text{pulse_doppler_signal}[i] \\ &\quad + \text{uwb_signal}[i] \end{aligned} \quad (28)$$

Hybrid Wi-Fi HaLow Radar Coverage: As discussed earlier, we consider numerous factors to determine the received power at a certain distance. These factors include the adjusted transmitted power, antenna gain, and the impact of attenuation, scattering, and fading caused by multiple material layers at that distance. The hybrid signal and other attenuation factors reduce the transmitted power. Finally, the resulting total power the hybrid radar system receives from the reflected signals after interacting with the debris consists of multiple layers is given below;

$$\begin{aligned} P_r &= P_t - G_A - \text{total_attenuation} - \text{total_scattering} \\ &\quad - \text{total_fading} - \text{integrated_signal}[i] \end{aligned} \quad (29)$$

Here, P_t , G_A are adjusted transmitted power and antenna gain in dBm and dBi, respectively. Moreover, *total_attenuation*, *total_scattering*, and *total_fading* are calculated for various materials and according to depth of debris. Radar coverage is established by computing signal strength at various distances. The coverage model integrates free-space path loss, where signal strength lessens exponentially with distance. The equation includes the term $-20 \cdot \log_{10}(\text{distance_range}[i])$ to adjust for this path loss, accentuating signal degradation as distance increases. The final radar coverage array represents

the strength of the Wi-Fi HaLow signal, subject to the effects of multilayered debris at varying distances.

$$\text{radar_coverage}[i] = P_r - 20 \cdot \log_{10}(\text{distance_range}[i]) \quad (30)$$

E. Debris Signal Loss

We need to carefully examine the losses experienced by the Wi-Fi Halow signal in our debris model, as it can be significantly damped by higher scattering, reflections, and fading. Existing statistical models could be more effective in this context, and redefining them specifically for collapsed structures is necessary. To address this, we will leverage the formulation found in existing literature and integrate them into our debris problem.

1. Attenuation Modeling:: The total attenuation (total_attenuation) at a specific distance for all material layers is the sum of individual material attenuations.

$$\text{total_attenuation} = \sum_{i=1}^N \alpha_i \times \text{distance_range}[i] \quad (31)$$

2. Scattering Modeling:: Scattering (total_scattering) is similarly modeled by summing up the product of scattering coefficients and distance, capturing the deviation of electromagnetic waves due to interactions with particles or irregularities in the material.

$$\text{total_scattering} = \sum_{i=1}^N \sigma_i \times \text{distance_range}[i] \quad (32)$$

3. Fading Modeling:: Incorporating stochastic elements such as fading into a simulation adds a layer of randomness, which can help better model real-world scenarios. Rayleigh fading [44], a widely accepted model for wireless communication scenarios, is utilized to introduce variability in the amplitude of the received signal.

$$f(x) = \frac{x}{\sigma^2} \exp\left(-\frac{x^2}{2\sigma^2}\right) \quad (33)$$

In the context of fading, x could be the fading factor (F) for a specific layer. The total fading (total_fading) at a specific distance for all material layers is the sum of individual material fadings.

$$\text{total_fading} = \sum_{i=1}^N F_i \times \text{distance_range}[i] \quad (34)$$

F. CSI Considerations

This study aims to examine the extent to which hybrid Wi-Fi Halow radar signals can be used in future SAR operations. This is made possible by the CSI [31] contained in the echo signal received from the debris model. However, the CSI may also include clutter and noise, leading to unreliable detection of vital signs. Thus, it is essential to incorporate robust sensing information in the CSI. As discussed in the echo model Section II-C, the echo signal must be above or equal to PDT to achieve this. Therefore, coverage is unreliable if the received power falls below a specific threshold (e.g., -70 dBm).

$$\text{if}(P_r - 20 \cdot \log_{10} \text{distance_range}[i]) < \text{threshold} \quad (35)$$

Algorithm 1 Simulation of Multilayered Debris

```

1: procedure SIMDEBRIS( $f_s, f_e, T_s, f_c, \text{PRF}, B, R$ )
   Input:
       $f_s$  - Start frequency of FMCW signal
       $f_e$  - End frequency of FMCW signal
       $T_s$  - Sweep time of FMCW signal
       $f_c$  - Center frequency of Pulse Doppler signal
      PRF - Pulse repetition frequency
      B - Bandwidth of UWB signal
      R - Number of rounds
   Output:
       $C_v$  - Signal coverage values
       $U_i$  - Indices of unreliable coverage
2: for  $r \leftarrow 1$  to  $R$  do
3:    $N_l \leftarrow \text{INPUT}(\text{"Round "r": Num layers: "})$ 
4:    $P \leftarrow \{\}, M \leftarrow []$ 
5:   for  $i \leftarrow 1$  to  $N_l$  do
6:      $L_n \leftarrow \text{INPUT}(\text{"Round "r": Material "}(i+1)\text{" ":"})$ 
7:      $M.append(L_n)$ 
8:      $S_c \leftarrow \text{INPUT}(\text{"Scattering for "}(L_n)\text{" :")}$ 
9:      $A_c \leftarrow \text{INPUT}(\text{"Attenuation for "}(L_n)\text{" :")}$ 
10:     $F_f \leftarrow \text{INPUT}(\text{"Fading for "}(L_n)\text{" :")}$ 
11:     $P[L_n] \leftarrow \{S_c, A_c, F_f\}$ 
12:   end for
13:    $N_s \leftarrow 1000$ 
14:    $D_r \leftarrow \text{np.linspace}(0.1, 10, N_s)$ 
15:    $P_t \leftarrow 17.0$ 
16:    $G_a \leftarrow 4.0$ 
17:    $S_1 \leftarrow \text{GenFMCW}(N_s, f_s, f_e, T_s, D_r)$ 
18:    $S_2 \leftarrow \text{GenPulseDoppler}(N_s, f_c, \text{PRF}, D_r)$ 
19:    $S_3 \leftarrow \text{GenUWB}(N_s, B, D_r)$ 
20:    $S_i \leftarrow S_1 + S_2 + S_3$ 
21:    $C_v \leftarrow \text{np.zeros}(N_s)$ 
22:    $U_i \leftarrow []$ 
23:   for  $j \leftarrow 1$  to  $N_s$  do
24:      $T_a \leftarrow 0.0, T_s \leftarrow 0.0, T_f \leftarrow 0.0$ 
25:     for  $L$ , Prop  $\leftarrow P.items()$  do
26:        $A_a \leftarrow \text{Prop}[0] \times D_r[j]$ 
27:        $T_a A_a$ 
28:        $A_s \leftarrow \text{Prop}[1] \times D_r[j]$ 
29:        $T_s A_s$ 
30:        $A_f \leftarrow \text{Prop}[2] \times D_r[j]$ 
31:        $T_f A_f$ 
32:     end for
33:      $P_r \leftarrow P_t - G_a - T_a - T_s - T_f - S_i[j]$ 
34:      $C_v[j] \leftarrow P_r - 20 \times \text{np.log10}(D_r[j])$ 
35:     if  $C_v[j] < -70$  then
36:        $U_i.append(j)$ 
37:     end if
38:   end for
39: end for
40: end procedure

```

G. Hybrid Wi-Fi Halow Radar Procedure

Our approach utilizes Algorithm 1 to implement the proposed solution. We begin by analyzing the critical attributes of each radar module, including start, end, and center frequencies, sweep time, bandwidth, PRF, and number of experiment rounds. Next, considering various materials and layer scenarios, we employ the debris model to map pancake or V-shaped collapsed structures. In addition, we consider stochastic variables such as attenuation, scattering, and fading coefficients from existing literature and model them to multilayered debris. From there, we compute individual FMCW,

PDR, and UWB components and integrate them to obtain the final signal at Wi-Fi HaLow frequency. Finally, we calculate the coverage range by accounting for received power and path loss, as discussed in Section III-D.

IV. SIMULATIONS AND RESULTS

This section presents our simulation method and numerical results for evaluation. We simulated Wi-Fi HaLow for our proposed hybrid radar mechanism. Firstly, we discuss the simulation methods, followed by results with comparative analysis.

A. Method

Ensuring the precise selection of simulation parameters to achieve significant results is paramount. In Table I, we have comprehensively displayed the requisite parameters. Furthermore, we utilized Python programming to perform our simulations on Jupiter Notebook, a widely recognized scientific computing platform.

Let's delve into the reasons behind our selection of simulation parameters. To begin with, we took into account the Wi-Fi HaLow frequency, which is set at 902MHz regulated by IEEE Task Group⁷ [6]. Additionally, we decided on a start and end frequency of 902MHz and 928MHz, respectively, for the FMCW module, while 910MHz was chosen as the center frequency as the average of extreme values. PRF is typically considered 500Hz to 1500Hz, but we assume it is for the pulse-doppler module at 1000Hz. Moreover, based on existing studies [21], we opted for a bandwidth of 750MHz for the UWB signal. Taking into account the Federal Communications Commission's(FCC) guidelines,⁸ we selected a transmitted power of 17dBm and antenna gain of 4dBi. We settled on a maximum receivable signal of -70dBm for better CSI.

Moving on to selecting debris types, we considered structural damages ranging from single-story to eight-story buildings with pancake and V-shaped collapse models. Based on case studies, we determined that single-story structures were typically made of mud or masonry, while multi-story structures were primarily composed of masonry debris. Mud debris consisted of rammed earth (RE), thatch (T.H.), stone (S), adobe brick (A.B.), and lumber (L), while masonry debris was mainly composed of concrete (C), brick (B), masonry block (M.B.), and lumber (L). These materials possess varying thickness levels, define the quality of construction, and have different scattering and attenuation coefficients and fading factors [45], as per Digi⁹ and U.S. National Institute of Standards and Technology's (NIST)¹⁰ findings. We consider pre-defined values of these structural components as research on structural materials in the context of CSI needs another investigation, which is not the scope of this article. Moreover, at the earlier stage of Wi-Fi sensing under debris, it can be tested with established literature.

TABLE I
SIMULATION PARAMETERS

Parameter	Values
Operational Frequencies Bandwidth for UWB Center Frequency Pulse Repetition Frequency	(902-928)MHz 750MHz 910MHz 1000Hz
Transmission Power Antenna Gain Signal PTD Number of Samples Sweep Time	17dBm 4dBi -70dBm 1000 0.1sec
Materials Types	Concrete, Brick, Masonry Block, Lumber Adobe Brick, Rammed Earth, Thatch, Stone
Scattering Coefficients	Concrete = C = 0.4-0.8 Brick = B = 0.3-0.6 Masonry Block= MB = 0.2-0.5 Lumber = L = 0.1-0.3 Adobe Brick = AB = 0.3-0.6 Rammed Earth = RE = 0.3-0.6 Thatch = TH = 0.1-0.3 Stone = S = 0.1-0.4
Attenuation Coefficients	Concrete = C = (0.2-0.8)dB/m Brick = B = (0.1-0.5)dB/m Masonry Block= MB = (0.1-0.4)dB/m Lumber = L = (0.05-0.2)dB/m Adobe Brick = AB = (0.2-0.5)dB/m Rammed Earth = RE = (0.2-0.5)dB/m Thatch = TH = (0.05-0.2)dB/m Stone = S = (0.1-0.4)dB/m
Fading Factor	Concrete = C = 0.8-0.95 Brick = B = 0.7-0.9 Masonry Block= MB = 0.7-0.9 Lumber = L = 0.6-0.8 Adobe Brick = AB = 0.7-0.9 Rammed Earth = RE = 0.7-0.9 Thatch = TH = 0.5-0.7 Stone = S = 0.6-0.8
Debris Scenarios Pancake	1-Story = 4 Layers (2C+MB+L) 1-Story = 4 Layers (2C+B+L) 1-Story = 7 Layers (2RE+2AB+3L) 1-Story = 7 Layers (2RE+2S+3L) 1-Story = 5 Layers (RE+TH+AB+2L) 1-Story = 5 Layers (RE+TH+S+2L) 2-Story = 8 Layers (4C+2MB+2L) 2-Story = 8 Layers (4C+2B+2L) 5-Story = 20 Layers (10C+5B+5L) 8-Story = 32 Layers (16C+8B+8L)
Debris Scenarios V-Shaped	1-Story = 4 Layers (RE+S+TH+L) 1-Story = 3 Layers (B+2C) 2-Story = 7 Layers (4C+B+2L) 5-Story = 18 Layers (10C+2B+6L)

B. Results

It's crucial to evaluate and compare the simulation results of the proposed Hybrid Wi-Fi HaLow Radar mechanism in terms of structural design and debris cases. We conducted thorough simulation tests on various debris scenarios from three seismic studies. The test encompassed 28 debris cases with varying materials and structures, ranging from single-story to multi-story collapses. It's fascinating that the survey revealed V-shaped collapses are possible up to 5-story structural collapses, while pancake collapses are evident in all structural damage. The detailed comparison results in Table II offer a comprehensive breakdown of the simulation outcomes based on four-floor layouts (1, 2, 5, and 8-story structures).

⁷http://www.ieee802.org/11/Reports/tgah_update.htm

⁸<https://www.fcc.gov/tags/radio-rules>

⁹<http://ftp1.digi.com/support/images/XST-AN005a-IndoorPathLoss.pdf>

¹⁰<https://www.nist.gov/mml/materials-data>

TABLE II
COVERAGE RANGE OF HYBRID WI-FI HALOW RADAR

Debris Thickness	Coverage Range in Debris (m) for (1,2,5,8) Story Structures													
	Zindajan (Afghanistan)-Balakot (Pakistan) Study								Yingxiu (China) Study					
	1-Story				2-Story				5 Story		8-Story			
	Pancake		V-Shaped		Pancake		V-Shaped		Pancake	V-Shaped	Pancake	Masonry		
Scenarios	C 1	C 2	C 3	C 4	C 5	C 6	C 7	C 8	C 9	C 10	C 11	C 12	C 13	C 14
Heavy	8.96	8.31	6.18	5.76	7.73	7.44	10+	8.63	4.20	4.16	5.31	1.83	2.06	1.19
Moderate	10+	9.85	7.20	6.76	9.43	9.30	10+	10+	5.17	5.05	6.96	2.29	2.51	1.50

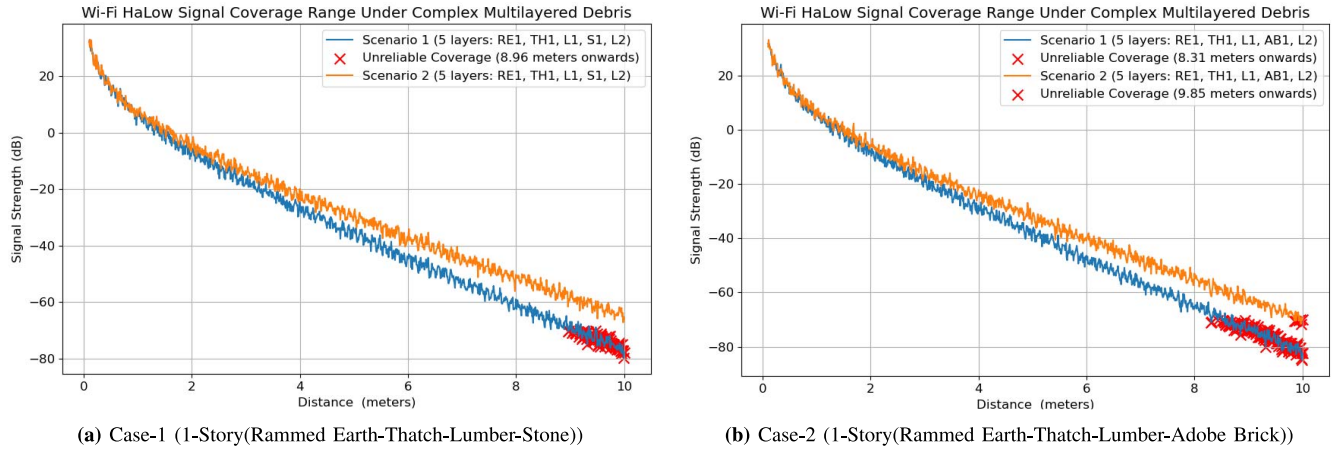


Fig. 7. 5-Layers Mud Pancake Debris, Simulation Study-1.

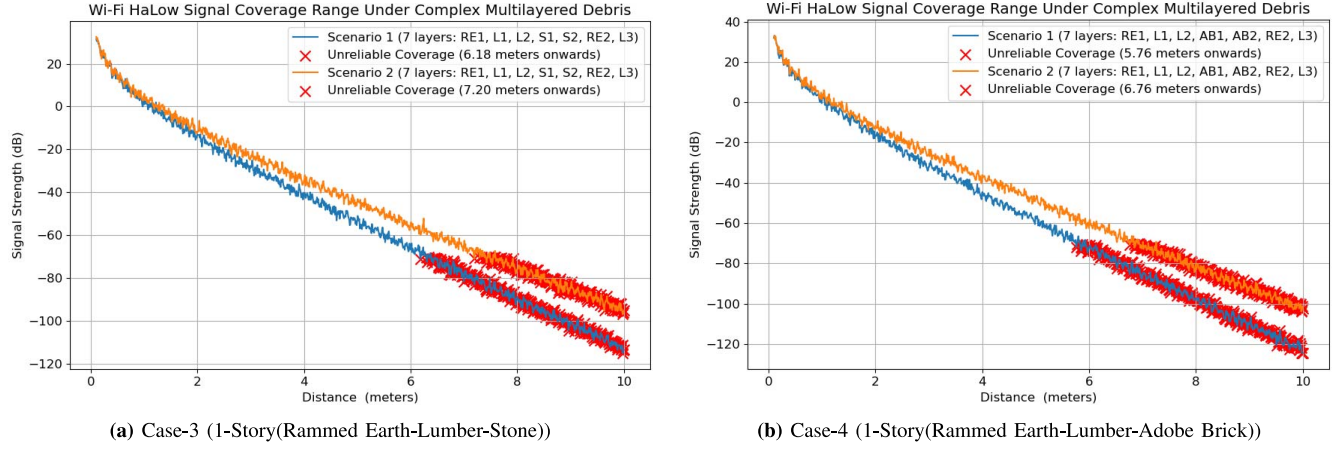


Fig. 8. 7-Layers Mud Pancake Debris, Simulation Study-2.

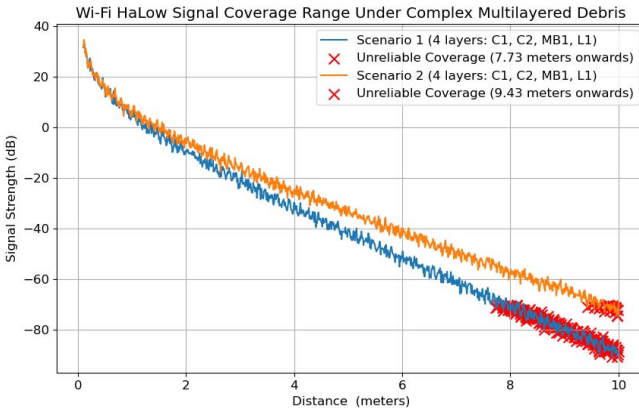
Therefore, in the forthcoming subsections, we will analyze and compare the simulation outcomes of the proposed Hybrid Wi-Fi HaLow Radar mechanism regarding structural layout and fall scenarios.

1) *Coverage W.R.T Single Story Pancake Debris:* Let us consider the simulation results of single-story pancake debris for six mud and masonry cases from Table II:

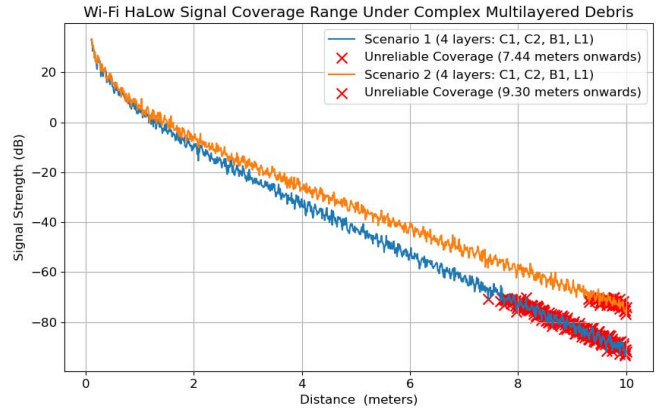
- Firstly, we study mud pancake structures, which are evident in Afghanistan and remote rural Pakistan. We observe that signal coverage under low-layered yet thick mud debris in study cases C1 (Rammed Earth, Thatch, Lumber, Stone) and C2 (Rammed Earth, Thatch, Lumber, Adobe Brick) is 8.96m and 8.31m, respectively, showing a falling trend due to the difference of signal behavior with stone and adobe brick, later bringing more losses

as shown in the Fig. 7 (7a, 7b). If we reduce the debris thickness for the same study cases, we get 10+m and 9.85m coverage for C1 and C2, respectively.

- Similarly, C3 (Rammed Earth, Lumber, Stone) and C4 (Rammed Earth, Lumber, Adobe Brick) for thick debris have coverage ranges of 6.18m and 5.76m, respectively. For the same study cases at moderate thickness, the range is 7.20m and 6.76m, respectively, as shown in Table II and Fig. 8 (8a, 8b).
- Moreover, we observe the same trend for masonry pancake collapse under study cases C5 (Concrete, Masonry Block, Lumber) and C6 (Concrete, Brick, Lumber) for thick and moderate debris by having ranges of 7.73m, 7.44m, 9.43m, and 9.30m, respectively, as shown in Fig. 9 (9a, 9b).

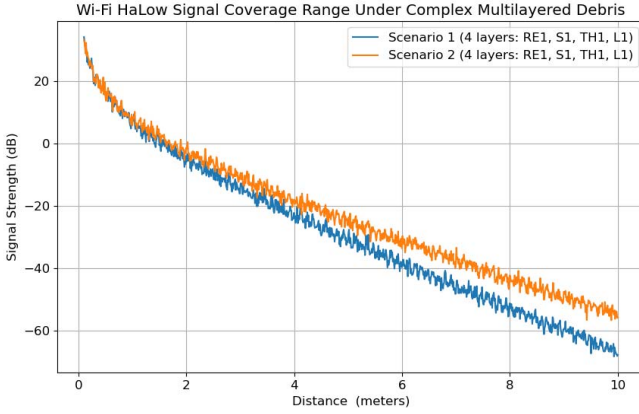


(a) Case-5 (1-Story(Concrete-Masonry Block-Lumber))

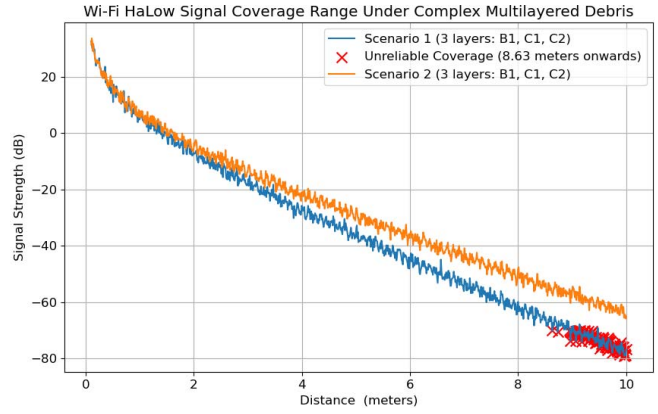


(b) Case-6 (1-Story(Concrete-Brick-Lumber))

Fig. 9. 4-Layers Masonry Pancake Debris, Simulation Study-3.



(a) Case-7 (1-Story(Rammed Earth-Thatch-Lumber-Stone)V)



(b) Case-8 (1-Story(Concrete-Brick)V)

Fig. 10. 3-4 Layers Masonry V-Shaped Debris, Simulation Study-4.

Therefore, it is concluded that with moderate debris thickness and low-layer scenarios for either mud or masonry structures, there is a chance of better Wi-Fi HaLow signal penetration with the proposed approach. However, as we tend to thick and high-layered rubble, coverage falls.

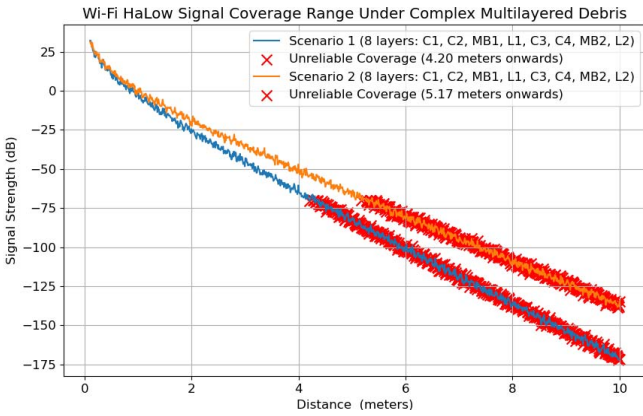
2) *Coverage W.R.T Single Story V-Shaped Debris:* Now, let us consider the V-shaped collapse of single-story mud and masonry study cases C7 (Rammed Earth, Stone, Thatch, Lumber) and C8 (Concrete, Brick) from Table II. We consider V-shaped collapse due to mud or weak masonry structures in developing countries, which form V shape on collapse and can lead to voids hence providing potential rescue chances.

- We observe that the coverage of the Wi-Fi HaLow signal for C7 under thick and moderate debris is above 10m in both cases, as shown in Fig. 10a, which is quite promising due to the nature of the collapse providing more room for open spaces and voids.
- Similarly, the C8 masonry study case for thick and moderate debris has coverage ranges of 8.63m and 10+m, respectively, as shown in Fig. 10b.

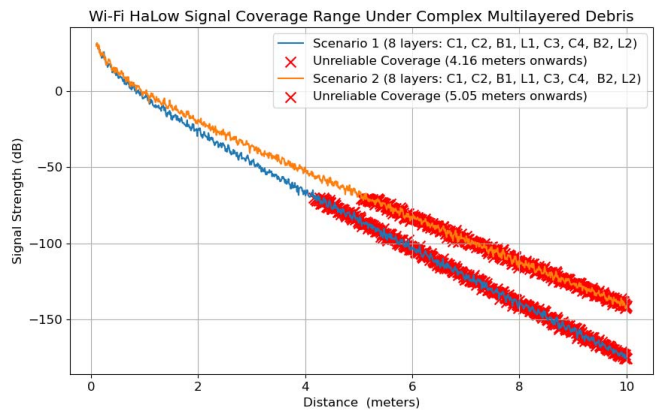
Therefore, it is concluded that with a V-shaped collapse for the mud study case, there is a chance of better Wi-Fi HaLow signal penetration with the proposed approach in comparison with masonry structures.

3) *Coverage W.R.T Double Story Pancake Debris:* Let's look closer at the Pancake collapse of double-story masonry study cases C9 (Concrete, Masonry Block, Lumber) and C10 (Concrete, Brick, Lumber), as listed in Table II. It's important to note that the Wi-Fi HaLow signal coverage for C9 differs depending on the debris thickness, with ranges of 4.20m and 5.17m for thick and moderate debris, respectively, as shown in Fig. 11a. Similarly, Fig. 11b displays coverage ranges of 4.16m and 5.05m for C10 under similar debris conditions. These results suggest that signal behavior varies between masonry blocks and brick, with the latter resulting in more significant losses. It's worth mentioning that our analysis only considers double-story masonry structures, as mud houses are generally single-story structures.

4) *Coverage W.R.T 2-5 Story V-Shaped Debris:* Let's examine the V-shaped collapse scenarios of double-story C11 (Concrete, Brick, Lumber) and five-story C13 (Concrete, Brick, Lumber) in Table II, specifically their Wi-Fi HaLow signal coverage. It's worth noting that the coverage for C11 follows a similar pattern as other scenarios listed above, with ranges of 5.31 and 6.96m for thick and moderate debris, respectively, as shown in Fig. 12a. Similarly, Fig. 12b shows that coverage ranges for C13 are 2.06m and 2.51m under similar debris conditions. These findings suggest that Wi-Fi

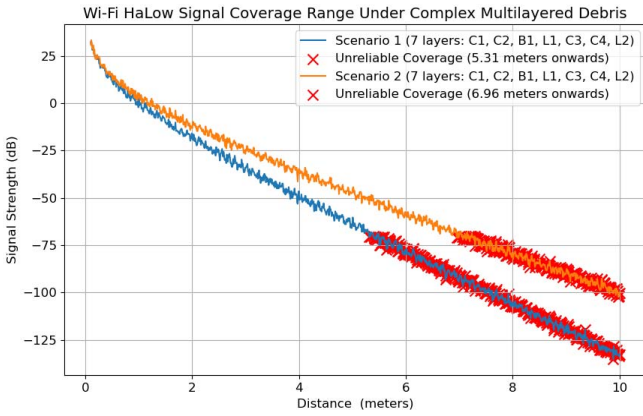


(a) Case-9 (2-Story(Concrete-Masonry Block-Lumber))

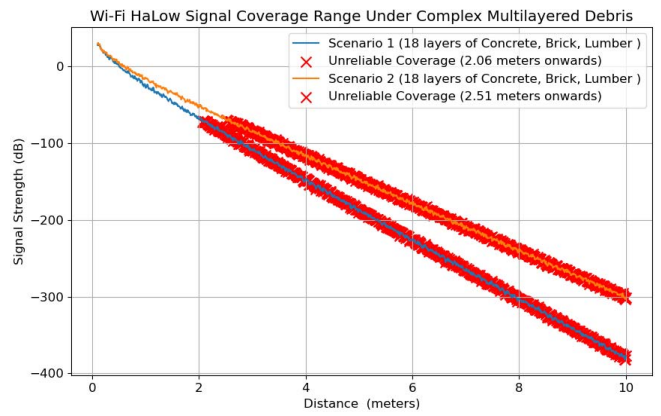


(b) Case-10 (2-Story(Concrete-Brick-Lumber))

Fig. 11. 8-Layers Masonry Pancake Debris, Simulation Study-5.



(a) Case-11 (2-Story(Concrete-Brick-Lumber)V)



(b) Case-13 (5-Story(Concrete-Brick-Lumber)V)

Fig. 12. 2-5 Layers Masonry V-Shaped Debris, Simulation Study-6.

HaLow signal losses are higher in C13 due to its 5-story structure, where debris forms higher rubble layers, making it more complex. Additionally, it's important to note that we only considered masonry structures for multi-floored scenarios, which are more common in China than in Afghanistan and Pakistan. Lastly, a V-shaped collapse still offers better coverage than a pancake collapse due to more voids and hanging rubble.

5) *Coverage W.R.T 5-8 Story Pancake Debris:* Finally, we study the Wi-Fi HaLow signal coverage in the context of pancake collapse scenarios for both C12 and C14, as enumerated in Table II. The examination reveals that C12's coverage follows a similar pattern to the abovementioned scenarios, with ranges of 1.83m and 2.29m for thick and moderate debris, respectively, as demonstrated in Fig. 13a. Similarly, Fig. 13b establishes that coverage ranges for C14 are 1.19m and 1.50m under similar debris conditions. These findings imply that Wi-Fi HaLow signal losses are more significant in C14 due to its 8-story structure, where debris forms higher rubble layers, making it more complex. Notably, the study only considered masonry structures for multi-floored scenarios, which are more prevalent in China than in Afghanistan and Pakistan. Lastly, it is worth noting that a pancake collapse results in more signal loss due to the higher debris layers.

V. PERFORMANCE ANALYSIS

In this segment, we provide a concise analysis of our study. Firstly, we consider the intricacy of the issue within the framework of existing literature. Next, we introduce a Hybrid Wi-Fi HaLow radar technique for ensuring coverage in collapsed structures. Lastly, we delve into this study's significance, potential applications, implications, and limitations..

When it comes to post-disaster rescue efforts, collapsed buildings present a complex challenge due to signal penetration issues. While radar sensing has been identified as the most viable technique [20], [21], [22], it requires adaptation to optimize its effectiveness. Unfortunately, expensive and impractical previous research I-A has hindered disaster management efforts, particularly in developing countries. To address this issue, our team previously proposed exploring using Wi-Fi radios as sensors to study coverage in collapsed structures [3], [4], [5]. Our approach leveraged previous studies to enhance cost-effectiveness and scalability. However, upon further examination, we realized that our last work needed more material modeling at each layer and Pulse-Doppler radar mapping to the Wi-Fi HaLow signal. We didn't explicitly employ the exact features of Pulse-Doppler radar, and no other study has yet explored this avenue regarding Wi-Fi signals.

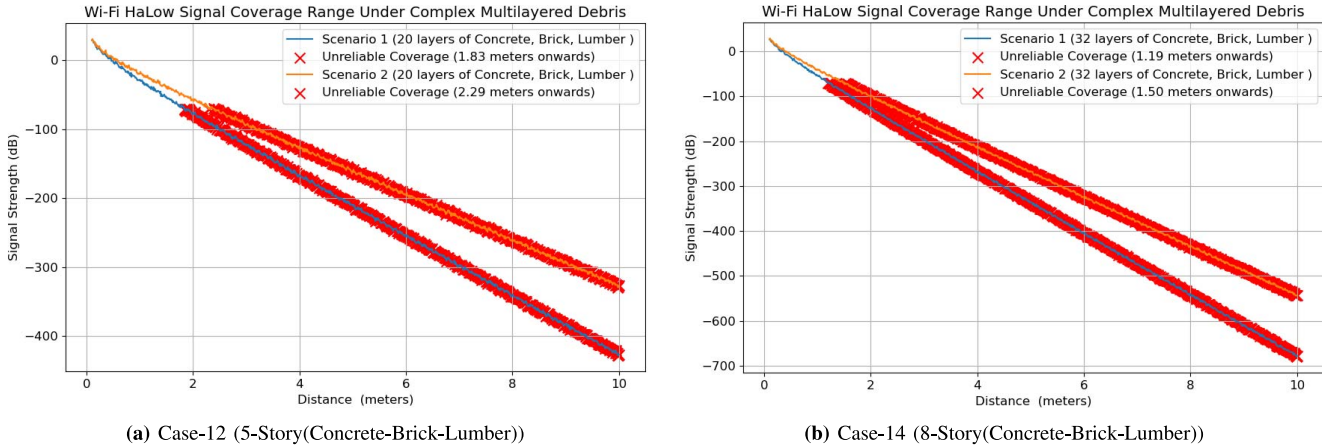


Fig. 13. 20-32 Layers Masonry Pancake Debris, Simulation Study-7.

Let's delve into our proposed Hybrid Wi-Fi HaLow radar technique. After thoroughly reviewing the existing literature, we found no research on hybrid radar techniques [39], [40] for SAR operation. However, previous studies have shown that GPR, Pulse Doppler Radar, UWB, and FMCW [20], [21], [22] have been individually tested for this purpose. We also discovered they had yet to explore these techniques with Wi-Fi signals or incorporate a hybrid approach. It's important to note that a single radar approach, regardless of type, cannot provide accurate results under collapsed structures. Furthermore, most existing radar works only focus on void detections or imaging solutions, which limits practicality. Our latest study introduces a Hybrid Wi-Fi HaLow radar that combines FMCW [35], [36], Pulse-doppler [37], [38], and UWB [21] radars to bring a unique and innovative approach to this field.

After examining the simulation results alongside our previous research, we refined our understanding of Wi-Fi HaLow radar coverage. While we had previously [3], [4], [5] determined that high antenna gains were necessary, our simulations yielded better results while considering practical antenna design limitations. Specifically, our hybrid proposal achieves optimal power at 17dBm with less antenna gain, making it a strong choice for coverage study in collapsed structures. We can maximize results in various scenarios by designing a hybrid transceiver that can switch between hybrid modules and fulfill the above antenna and power requirements. In addition, our research indicates that signal coverage is often better in mud structures, which are commonly found in weaker economies needing proper civil engineering structures. This is especially important given the potential for even small-magnitude events to cause significant loss of life. By utilizing a ubiquitous Wi-Fi-based solution, SAR operations can be expedited, and better coverage can be achieved in smaller structures.

Limitations: As with any research, this study has its limitations. One significant limitation is that we confined ourselves to simulations and have yet to implement the proposed hybrid Wi-Fi HaLow radar method in field surveys. However, this is simply due to the early stage of our work, and simulations are an essential first step before practical deployment. Additionally, our technique utilized an environmental loss

model, which may only be partially feasible due to practical factors such as fading, scattering, noise, and clutter. Nevertheless, we are confident that we will achieve better coverage since Digi, NIST, and other studies have already estimated the values of channel factors for various debris materials. It's important to note that our study's scope was to investigate the potential of a hybrid Wi-Fi HaLow radar mechanism. Therefore, we opted to use existing practical deployment values instead of simulating channel loss factors, which would only provide theoretical results. A practical study on attenuations, losses, fading, and related phenomena is necessary to deploy the Wi-Fi sensing solution practically. Nevertheless, our work will ignite research into addressing multipath fading, scattering, and other associated challenges to increase Wi-Fi signal strength.

Impact: The findings of this research have significant implications for disaster response and public safety. Our hybrid radar-Wi-Fi HaLow system enhances signal penetration in collapsed structures. This method has the potential to be integrated into emergency response protocols, providing a reliable tool for locating individuals in debris. Furthermore, our discoveries could impact the design of future IoT-based sensing systems, advocating for low-frequency Wi-Fi standards to ensure better coverage and reliability in complex environments. This research addresses current limitations in wireless sensing technologies and paves the way for more resilient and effective disaster management solutions.

VI. CONCLUSION

Our research explored the viability of using a blend of FMCW, Pulse-doppler, and UWB radar technologies to establish reliable Wi-Fi HaLow coverage in collapsed buildings. Our focus was on earthquake scenarios, and we analyzed the indoor layouts of three different sites in various countries to understand better the signal penetration challenges posed by multi-layered and multi-obstacle environments. We then presented a signal propagation mechanism that adapts sub-1GHz Wi-Fi HaLow frequencies to utilize the three radar signals effectively. Our simulations showed that this innovative hybrid approach can offer superior coverage compared to existing studies. We also found that our methodology benefits

low-layered debris with mud structures. However, further improvements are needed to address complex channel factors, such as fading, scattering, and multipath analysis, in multi-floor masonry structures.

REFERENCES

- [1] J. Xiao, H. Li, M. Wu, H. Jin, M. J. Deen, and J. Cao, "A survey on wireless device-free human sensing: Application scenarios, current solutions, and open issues," *ACM Comput. Surv.*, vol. 55, no. 5, pp. 1–35, 2023.
- [2] J. C. Soto, I. Galdino, E. Caballero, V. Ferreira, D. Muchaluat-Saade, and C. Albuquerque, "A survey on vital signs monitoring based on Wi-Fi CSI data," *Comput. Commun.*, vol. 195, pp. 99–110, Nov. 2022.
- [3] M. F. Khan, G. Wang, M. Z. A. Bhuiyan, and K. Yang, "Toward Wi-Fi Halow signal coverage modeling in collapsed structures," *IEEE Internet Things J.*, vol. 7, no. 3, pp. 2181–2196, Mar. 2020.
- [4] M. F. Khan, G. Wang, and M. Z. A. Bhuiyan, "Towards debris information analysis and abstraction for Wi-Fi radar edge in collapsed structures," *IEEE Access*, vol. 7, pp. 168075–168090, 2019.
- [5] M. F. Khan, G. Wang, and M. Z. A. Bhuiyan, "Wi-Fi frequency selection concept for effective coverage in collapsed structures," *Future Gener. Comput. Syst.*, vol. 97, pp. 409–424, Aug. 2019.
- [6] *IEEE Recommended Practice For Local and Metropolitan Area Networks—Part 19: Coexistence Methods for IEEE 802.11 and IEEE 802.15.4 Based Systems Operating in the Sub-1 GHz Frequency Bands*, IEEE Standard 802.19.3-2021, 2021, pp. 1–79.
- [7] K. Singh, P.-C. Wang, S. Biswas, S. K. Singh, S. Mumtaz, and C.-P. Li, "Joint active and passive beamforming design for RIS-aided IBFD IoT communications: QoS and power efficiency considerations," *IEEE Trans. Consum. Electron.*, vol. 69, no. 2, pp. 170–182, May 2023.
- [8] S. Li, C. Gao, M. Wei, J. Zhao, P. Shao, and J. Xu, "CSI-impaired secure resource allocation for SWIPT-enabled full-duplex consumer Internet of Things networks in smart healthcare," *IEEE Trans. Consum. Electron.*, vol. 69, no. 4, pp. 685–696, Nov. 2023.
- [9] C. K. Wu, C.-T. Cheng, Y. Uwate, G. Chen, S. Mumtaz, and K. F. Tsang, "State-of-the-art and research opportunities for next-generation consumer electronics," *IEEE Trans. Consum. Electron.*, vol. 69, no. 4, pp. 937–948, Nov. 2023.
- [10] Z. Guan et al., "ECOSECURITY: Tackling challenges related to data exchange and security: An edge-computing-enabled secure and efficient data exchange architecture for the energy Internet," *IEEE Consum. Electron. Mag.*, vol. 8, no. 2, pp. 61–65, Mar. 2019.
- [11] C. Kim, S. Jang, and J.-B. Chung, "Differences between the effects of direct and indirect earthquake experiences on disaster preparedness," *Nat. Hazards Rev.*, vol. 25, no. 1, 2024, Art. no. 05023015.
- [12] M. Pardo Rios et al., "Urban search and rescue operations USAR in collapsed buildings after the 2023 earthquake in Turkiye," *Emergencias*, vol. 35, no. 4, pp. 288–296, 2023.
- [13] S. Rasakatla, W. Tenma, T. Suzuki, B. Indurkhya, and I. Mizuuchi, "CameraRoach: A WiFi- and camera-enabled cyborg cockroach for search and rescue," *J. Robot. Mechatron.*, vol. 34, no. 1, pp. 149–158, 2022.
- [14] G. Wang et al., "Development of a search and rescue robot system for the underground building environment," *J. Field Robot.*, vol. 40, no. 3, pp. 655–683, 2023.
- [15] S. Han et al., "Snake robot gripper module for search and rescue in narrow spaces," *IEEE Robot. Autom. Lett.*, vol. 7, no. 2, pp. 1667–1673, Apr. 2022.
- [16] E. Sahin, M. A. Akkas, and O. Dagdeviren, "Nanonetwork-based search and rescue operations in debris areas," *Comput. Netw.*, vol. 237, Dec. 2023, Art. no. 110082.
- [17] J. Bravo-Arrabal, P. Zambrana, J. J. Fernandez-Lozano, J. A. Gomez-Ruiz, J. S. Barba, and A. Garcia-Cerez, "Realistic deployment of hybrid wireless sensor networks based on ZigBee and LoRa for search and rescue applications," *IEEE Access*, vol. 10, pp. 64618–64637, 2022.
- [18] A. Depold, C. Dorn, S. Erhardt, R. Weigel, and F. Lurz, "A direction-of-arrival estimation system for UAV-assisted search and rescue: Locating mobile phones to improve the survival chance of disaster victims," *IEEE Microw. Mag.*, vol. 24, no. 3, pp. 59–64, Mar. 2023.
- [19] A. Albanese, V. Sciancalepore, and X. Costa-Pérez, "SARDO: An automated search-and-rescue drone-based solution for victims localization," *IEEE Trans. Mobile Comput.*, vol. 21, no. 9, pp. 3312–3325, Sep. 2022.
- [20] D. Hu, L. Chen, J. Du, J. Cai, and S. Li, "Seeing through disaster rubble in 3D with ground-penetrating radar and interactive augmented reality for urban search and rescue," *J. Comput. Civ. Eng.*, vol. 36, no. 5, 2022, Art. no. 04022021.
- [21] A. Sarkar and D. Ghosh, "Accurate sensing of multiple humans buried under rubble using IR-UWB SISO radar during search and rescue," *Sens. Actuat. A Phys.*, vol. 348, Dec. 2022, Art. no. 113975.
- [22] D. Hu, J. Chen, and S. Li, "Reconstructing unseen spaces in collapsed structures for search and rescue via deep learning based radargram inversion," *Autom. Construct.*, vol. 140, Aug. 2022, Art. no. 104380.
- [23] M. Cominelli, F. Gringoli, and F. Restuccia, "Exposing the CSI: A systematic investigation of CSI-based Wi-Fi sensing capabilities and limitations," in *Proc. IEEE Int. Conf. Pervasive Comput. Commun. (PerCom)*, 2023, pp. 81–90.
- [24] Z. Jiang et al., "Eliminating the barriers: Demystifying Wi-Fi baseband design and introducing the PicoScenes wi-Fi sensing platform," *IEEE Internet Things J.*, vol. 9, no. 6, pp. 4476–4496, Mar. 2022.
- [25] J. Guo, I. W.-H. Ho, Y. Hou, and Z. Li, "FedPos: A federated transfer learning framework for CSI-based Wi-Fi indoor positioning," *IEEE Syst. J.*, vol. 17, no. 3, pp. 4579–4590, Sep. 2023.
- [26] D. Konings, R. Grace, and F. Alam, "A stacked neural network-based machine learning framework to detect activities and falls within multiple indoor environments using Wi-Fi CSI," *IEEE Sensors Lett.*, vol. 5, no. 5, pp. 1–4, May 2021.
- [27] Z. Guo, X. Zhu, L. Gui, B. Sheng, and F. Xiao, "BreathID: Respiration sensing for human identification using commodity Wi-Fi," *IEEE Syst. J.*, vol. 17, no. 2, pp. 3059–3070, Jun. 2023.
- [28] Y. Yin, X. Yang, J. Xiong, S. I. Lee, P. Chen, and Q. Niu, "Ubiquitous smartphone-based respiration sensing with Wi-Fi signal," *IEEE Internet Things J.*, vol. 9, no. 2, pp. 1479–1490, Jan. 2022.
- [29] Y. Gu et al., "Secure user authentication leveraging keystroke dynamics via Wi-Fi sensing," *IEEE Trans. Ind. Informat.*, vol. 18, no. 4, pp. 2784–2795, Apr. 2022.
- [30] M. Cominelli, F. Gringoli, and R. Lo Cigno, "AntiSense: Standard-compliant CSI obfuscation against unauthorized Wi-Fi sensing," *Comput. Commun.*, vol. 185, pp. 92–103, Mar. 2022. [Online]. Available: <https://www.sciencedirect.com/science/article/pii/S0140366421004916>
- [31] W. Li, M. J. Bocus, C. Tang, R. J. Piechocki, K. Woodbridge, and K. Chetty, "On CSI and passive Wi-Fi radar for opportunistic physical activity recognition," *IEEE Trans. Wireless Commun.*, vol. 21, no. 1, pp. 607–620, Jan. 2022, doi: [10.1109/TWC.2021.3098526](https://doi.org/10.1109/TWC.2021.3098526).
- [32] F. Di Trapani, A. P. Sberna, M. Di Benedetto, S. Villar, C. Demartino, and G. C. Marano, "Dynamic progressive collapse response of multi-storey frame structures with masonry infills," *Structures*, vol. 54, pp. 1336–1349, Aug. 2023.
- [33] A. B. Torghabeh, M. Tehrani-zadeh, and A. Taslimi, "Probability of collapse evaluation for high-rise reinforced concrete buildings in the event of near-fault earthquakes and soil-structure interaction effects," *Structures*, vol. 55, pp. 1675–1691, Sep. 2023.
- [34] Y. Huo, Y. Xu, X. Zhao, Y. Sun, and S. Li, "Path loss estimation of wireless sensor networks in coal mine collapsed zone," *IEEE Sensors J.*, vol. 24, no. 6, pp. 9002–9015, Mar. 2024.
- [35] S. Gong et al., "Human activity recognition with FMCW radar using few-shot learning," *IEEE Sensors J.*, vol. 23, no. 15, pp. 17815–17824, Aug. 2023.
- [36] W. Xue, R. Wang, L. Liu, and D. Wu, "Accurate multi-target vital signs detection method for FMCW radar," *Measurement*, vol. 223, Dec. 2023, Art. no. 113715.
- [37] T. Schöffl, G. Nagl, R. Koschuch, H. Schreiber, J. Hubl, and R. Kaitna, "A perspective of surge dynamics in natural debris flows through pulse-Doppler radar observations," *J. Geophys. Res.-Earth Surf.*, vol. 128, no. 9, 2023, Art. no. e2023JF007171.
- [38] T. Miwa and Y. Nakazawa, "Nondestructive evaluation of localized rebar corrosion in concrete using vibro-radar based on pulse Doppler imaging," *Remote Sens.*, vol. 14, no. 18, p. 4645, 2022.
- [39] H. Zhou, C. Peng, K. Guo, Y. Lei, and Z. Guo, "Estimating parameters of ballistic target by single hybrid radar based on vortex and wideband electromagnetic waves," *IEEE Sensors J.*, vol. 23, no. 21, pp. 26423–26429, Nov. 2023.
- [40] M.-S. Jung, J.-H. Choi, M.-S. Song, J.-E. Roh, and K.-T. Kim, "Design of a hybrid radar sensor to monitor the behavior of a projectile in a circular tube," *IEEE Access*, vol. 11, pp. 123650–123658, 2023.
- [41] T.-F. Liu, "Digital signal processing for the detection of hidden objects using an FMCW radar," M.S. thesis, Dept. Electron. Eng., Queen Mary Univ. London, London, U.K., 1987.

- [42] J. K. Glazner, *Ranging Performance of A Pulse Doppler Radar*. Arlington, TX, USA: Univ. Texas Arlington, 1988.
- [43] R. Kapoor, A. Banerjee, G. Tsihrintzis, and N. Nandhakumar, "UWB radar detection of targets in foliage using alpha-stable clutter models," *IEEE Trans. Aerosp. Electron. Syst.*, vol. 35, no. 3, pp. 819–834, Jul. 1999.
- [44] S. Saha, "Detection of Rayleigh faded signals using two distributed sensors," M.S. thesis, Univ. Mississippi, Oxford, MS, USA, 2023.
- [45] T. S. Rappaport et al., "Millimeter wave mobile communications for 5G cellular: It will work!" *IEEE Access*, vol. 1, pp. 335–349, 2013.



Muhammad Faizan Khan received the B.E. degree in information and communication system engineering from the National University of Science and Technology, Pakistan, in 2012, the M.S. degree in communication and information systems from the Huazhong University of Science and Technology, in 2014, and the Ph.D. degree in cyberspace security from Guangzhou University, China, in 2019, where he is currently working as a Postdoctoral Fellow with the School of Computer Science and Cyber Engineering. Moreover, he is also an Assistant Professor, and a Doctoral Supervisor with the Department of Information Technology, The University of Haripur, Pakistan. His research interests include signal kinetics, Wi-Fi sensing, IoT, and cyberspace security.



Guojun Wang (Member, IEEE) received the B.Sc. degree in geophysics, and the M.Sc. and Ph.D. degrees in computer science from the Central South University of Technology in 1992, 1996, and 2002, respectively. He is a Pearl River Scholarship Distinguished Professor of Higher Education in Guangdong Province, and a Doctoral Supervisor with the School of Computer Science and Cyber Engineering, Guangzhou University, China. Before joining Guangzhou University, he was a Professor with Central South University, an Adjunct Professor with Temple University, USA, a Visiting Scholar with Florida Atlantic University, USA, a Visiting Researcher with the University of Aizu, Japan, and a Research Fellow with The Hong Kong Polytechnic University. He has been listed in Chinese Most Cited Researchers (Computer Science/Cyberspace Security) by Elsevier in the past 10 consecutive years from 2014 to 2023. His h-index is 67 (as of the date 14 May 2024). His research interests include artificial intelligence, blockchain, cloud computing, trustworthy/dependable computing, cyberspace security, and recommendation systems. He is a Distinguished Member of CCF and a member ACM and IEICE. For more information, see <http://trust.gzhu.edu.cn/faculty/csgjwang/>.



Zhigao Zheng (Member, IEEE) is with Wuhan University. He published more than 20 peer-reviewed publications (such as the *IEEE TRANSACTIONS ON PARALLEL AND DISTRIBUTED SYSTEMS* and *IEEE TRANSACTIONS ON COMPUTERS*). He joins research projects from various governmental and industrial organizations, such as the National Science Foundation of China, the Ministry of Science and Technology, and the Ministry of Education. His current research interests focus on cloud computing, big data processing, and AI systems. He is an Executive Committee Member of the Technical Committee on Distributed Computing Systems and Embedded Systems of CCF. He is also an Editorial Board Member of some high quality journals, such as the *IEEE TRANSACTIONS ON CONSUMER ELECTRONICS* and *Mobile Networks and Applications*. He is a PC Member of several Top conferences, such as TheWebConf (formally WWW) and NeurIPS, and the Vice PC Chair of CPSCom 2023. He is a member of ACM and CCF.



Xiangyong Liu received the Ph.D. degree in computer science from Central South University, China, in 2021. He is currently a Postdoctoral Fellow with the School of Computer Science, Guangzhou University. His research interests include blockchain security, mobile security, and recommender system.